



DNase-dependent, NET-independent pathway of thrombus formation in vivo

Estelle Carminita^a, Lydie Crescence^{a,b} , Nicolas Brouilly^c, Alexandre Altié^a , Laurence Panicot-Dubois^{a,b}, and Christophe Dubois^{a,b,1} 

^aAix Marseille University, INSERM 1263, Institut National de la Recherche pour l'Agriculture, l'Alimentation et l'Environnement (INRAE) 1260, Center for CardioVascular and Nutrition Research (C2VN), 13380 Marseille, France; ^bAix Marseille University, Plateforme d'Imagerie Vasculaire et de Microscopie Intravital, C2VN, 13380 Marseille, France; and ^cCNRS UMR 7288, Institut de Biologie du Développement de Marseille, 13288 Marseille, France

Edited by David Ginsburg, University of Michigan–Ann Arbor, Ann Arbor, MI, and approved May 24, 2021 (received for review January 18, 2021)

The contribution of NETs (neutrophil extracellular traps) to thrombus formation has been intensively documented in both arterial and venous thrombosis in mice. We previously demonstrated that adenosine triphosphate (ATP)-activated neutrophils play a key role in initiating the tissue factor-dependent activation of the coagulation cascade, leading to thrombus formation following laser-induced injury. Here, we investigated the contribution of NETs to thrombus formation in a laser-induced injury model. In vivo, treatment of mice with DNase-I significantly inhibited the accumulation of polymorphonuclear neutrophils at the site of injury, neutrophil elastase secretion, and platelet thrombus formation within seconds following injury. Surprisingly, electron microscopy of the thrombus revealed that neutrophils present at the site of laser-induced injury did not form NETs. In vitro, ATP, the main neutrophil agonist present at the site of laser-induced injury, induced the overexpression of PAD4 and CitH3 but not NETosis. However, compared to no treatment, the addition of DNase-I was sufficient to cleave ATP and adenosine diphosphate (ADP) in adenosine. Human and mouse platelet aggregation by ADP and neutrophil activation by ATP were also significantly reduced in the presence of DNase-I. We conclude that following laser-induced injury, neutrophils but not NETs are involved in thrombus formation. Treatment with DNase-I induces the hydrolysis of ATP and ADP, leading to the generation of adenosine and the inhibition of thrombus formation in vivo.

thrombosis | NETs | neutrophil | adenosine | intravital microscopy

Thrombosis is one of the major causes of human mortality. Ischemic stroke, myocardial infarction, and pulmonary embolism are the most common thrombotic complications. Platelets have been described as the main drivers of thrombosis. Activated platelets directly participate in thrombus formation by interacting with fibrinogen, secreting different platelet agonists and participating in activation of the blood coagulation cascade. Recently, neutrophils in addition to platelets were described to play an important role in thrombus formation in both the arteries and veins. We previously showed that in a laser-induced injury model, neutrophils are the first cells present at the site of injury. Neutrophils interact with the injured vessel wall are activated by adenosine triphosphate (ATP) and generate tissue factor (TF) on their surface, leading to the generation of thrombin, which is involved in the recruitment of platelets (1, 2).

Activated neutrophils have also been found to play an important role in the veins in a deep vein thrombosis (DVT) model through the secretion of neutrophil elastase (NE), leading to the degradation of TF pathway inhibitor (TFPI) and sustained activity of TF at the site of injury (3, 4). Once activated, neutrophils may produce neutrophil extracellular traps (NETs). NETosis involves different reactive oxygen species (ROS)-dependent and ROS-independent intracellular pathways and leads to decondensation of DNA by different histone deaminases and secretion of DNA and various proteins, such as the histones and enzymes originally present in neutrophil granules. NETosis involves different intracellular pathways depending on the neutrophil agonists used (5). The most commonly used agonists are phorbol myristate acetate (PMA), calcium ionophore,

lipopolysaccharide (LPS), and bacteria (*Streptococcus agalactiae*), which have been shown to induce NETs within a few hours. ROS generation, the family of peptidyl arginine deiminase (PAD) enzymes, and neutrophil serine proteases such as NE are differentially required by different stimuli (6). The intracellular pathways may be dependent on ROS generation by NADPH oxidase and/or on histone citrullination by PAD4, MPO, and NE (7). In all cases, NETs produced upon stimulation are proteolytically active, kill bacteria, and are composed mainly of chromosomal DNA and proteins originally present in neutrophil granules.

In vitro studies have shown that NETs may participate in platelet aggregation and activation of the blood coagulation cascade. Indeed, NETs are involved in thrombosis in several ways. NETs form scaffolds for the adhesion of platelets, red blood cells, and platelet adhesion molecules (fibrinogen, fibronectin, and von Willebrand factor [vWF]) (8). Moreover, these scaffold components trigger platelet activation and blood coagulation. For instance, histones such as histones H3 and H4 can interact with platelets via fibrinogen (9) or Toll-like receptor (TLR) 2 and 4 (10), resulting in platelet aggregation and thrombin generation (11). Additionally, neutrophil serine proteases such as NE, MPO, and cathepsin G enhance both the extrinsic coagulation pathway via proteolysis of TFPI (12) and the intrinsic coagulation pathway by binding and activating FXII (13). Although it is difficult to distinguish NETs from activated neutrophils in vivo, the main proof of concept that NETs indeed play a role in thrombus formation has come from experiments using DNase-I in mice. In a DVT model, injection of 100 U DNase-I significantly reduces the size of the thrombus (13).

Significance

Thrombosis constitutes a major contributor to the global disease burden. Recently, the contribution of neutrophils and neutrophil extracellular traps in thrombosis has been intensively documented. DNase-I by its ability to cleave DNA has been proposed as an efficient antithrombotic drug. In this paper, we showed that DNase-I inhibits the formation of a platelet thrombus and the generation of fibrin independent of its enzymatic activity on DNA. We proposed that DNase-I hydrolyzes adenosine triphosphate and adenosine diphosphate (two important platelet and neutrophil agonists) into adenosine, an antagonist of platelet and neutrophil.

Author contributions: E.C., L.P.-D., and C.D. designed research; E.C., L.C., N.B., and A.A. performed research; E.C., L.C., N.B., A.A., L.P.-D., and C.D. analyzed data; L.C. contributed new reagents/analytic tools; and L.P.-D. and C.D. wrote the paper.

The authors declare no competing interest.

This article is a PNAS Direct Submission.

Published under the PNAS license.

¹To whom correspondence may be addressed. Email: christophe.dubois@univ-amu.fr.

This article contains supporting information online at <https://www.pnas.org/lookup/suppl/doi:10.1073/pnas.2100561118/-DCSupplemental>.

Published July 6, 2021.

Since activated neutrophils are key cells involved in thrombus formation following laser-induced injury, the aim of the present study was to identify the role played by NETs in this model. We first used wild-type (WT) mice treated (or not) with DNase-I to investigate the role of NETs *in vivo* in a laser-induced model of thrombosis. We found that infusion of DNase-I into mice decreased thrombus growth, fibrin generation, neutrophil recruitment, and elastase release at the site of injury. However, surprisingly, we were not able to detect NETs at the site of thrombosis by electron microscopy. In contrast, we observed that DNase-I hydrolyzed ATP into adenosine diphosphate (ADP) and ADP into adenosine. Interestingly, both ATP and ADP are agonists of neutrophils and platelets, whereas adenosine inhibits neutrophil activation.

In conclusion, we propose that DNase-I hydrolyzes ATP and ADP and induces adenosine production, leading to the inhibition of thrombus formation *in vivo*.

Results

DNase-I Inhibits Thrombus Formation after Laser-Induced Injury. We previously demonstrated that the accumulation of activated neutrophils in the vessel wall following laser-induced injury is required for thrombosis (2). To determine the involvement of NETs in thrombus formation following laser-induced injury, we first compared the kinetics of platelet and fibrin accumulation in mice treated or not with DNase-I. As previously described in WT control mice, after laser-induced injury, platelets adhered and accumulated rapidly at the site of injury, contributing to the early phase of thrombus formation. The platelet thrombus grew rapidly to its maximum size between 80- and 120-s postinjury and then decreased in size. Fibrin was constantly generated at the site of injury (Fig. 1A, *Upper Panel*). Compared to no treatment, infusion of 100 U DNase-I, corresponding to ~ 0.05 U/ μ L DNase-I (13), led to decreased platelet accumulation and fibrin generation after vessel wall injury (Fig. 1A, *Lower Panel*). Quantitative data were obtained by analyzing multiple thrombi of mice treated or not with DNase-I. The accumulation of platelets was strongly decreased (Fig. 1B) by up to 65% (Fig. 1C) when DNase-I was infused into the bloodstream compared to when no treatment was administered. Similarly, compared to no treatment, infusion of DNase-I resulted in a significant reduction in fibrin generation (Fig. 1D) by up to 52% (Fig. 1E). Infusion of 100 U DNase-I into mice also led to a significant decrease in neutrophil accumulation after vessel wall injury (Fig. 2A) by up to 89% (Fig. 2B and C) compared to that observed after no treatment. As suspected, NE release was significantly decreased (Fig. 2D) by up to 53% (Fig. 2E and F) after infusion of DNase-I into the bloodstream compared to the control condition. Altogether, these results indicate that infusion of DNase-I significantly affects thrombus formation, neutrophil accumulation and activation, and ultimately fibrin generation following laser-induced injury.

In vivo, we observed that DNase-I strongly affects thrombus formation in the seconds following injury. However, as described previously using purified neutrophils (human and mouse), *in vitro* NETs formation following activation by 25 μ M platelet-activating factor (PAF) or 50 nM PMA (following priming with 2 ng/mL TNF- α) (Fig. 3A, *Left and Right Panels*) is only observed after 3 h. Interestingly, when ATP or ADP, both of which are triggers of thrombus formation in the laser-induced injury model, were used *in vitro*, no NETs formed, even when neutrophils were primed with 2 ng/mL TNF- α (Fig. 3B and C). These results were confirmed with human neutrophils (Fig. 3D and E). Detection of histone H3 citrullination (CitH3) by active PAD4 is commonly used to characterize NET formation. Although no NETs were formed, we observed the expression of both CitH3 (Fig. 4A and B) and PAD4 (Fig. 4C and D) following activation of resting neutrophils with 25 μ M ATP for 1 h. These results were confirmed by immunoblotting techniques (Fig. 4E–J). We observed an overexpression of PAD4 (Fig. 4E and H), CitH3 (Fig. 4F and I), and

NE (Fig. 4G and J) following activation of neutrophils by ATP. These results indicate that neither ATP- nor ADP-induced NETosis. PAD4, CitH3, and NE cannot be considered markers of NETosis but are rather markers of neutrophil activation. Taken together, our results suggest that *in vivo*, either NETs are preformed, circulate in the bloodstream and accumulate at the site of laser injury in the seconds following the formation of the thrombus, or that DNase-I inhibits thrombus formation independently of NETs formation.

Neutrophils but Not NETs Are Present at the Site of Laser-Induced Injury. To detect the presence of NETs in a thrombus following laser-induced injury, we first performed *in vitro* electron microscopy experiments on purified neutrophils. Scanning electron microscopy (SEM) revealed a granulating and burgeoning membrane of PAF-activated neutrophils forming NETs with expelled DNA fibers not observed in resting nonactivated neutrophils (Fig. 5A, *Upper Panel*). Transmission electron microscopy (TEM) showed that the observed resting neutrophils contained DNA had an intact plasma membrane and exhibited no DNA fibers. In contrast, PAF-activated neutrophil-secreting NETs expelled DNA fibers, had disrupted plasma membranes, and contained many more granules than nonactivated cells (Fig. 5A, *Lower Panel*). We next examined a cremaster arteriole containing a laser-induced platelet thrombus by TEM. In accordance with our previous descriptions, a neutrophil (N) interaction with the injured endothelial cells (E) and platelets (P) forming the thrombus was observed at the site of injury. Four different fields spaced 1 μ m from the neutrophil were examined by TEM to detect the presence of DNA fibers outside the cell (Fig. 5B, *Upper Panel*). The neutrophil observed at the site of injury contained DNA, the plasma membrane was intact, and exhibited no DNA fibers, strongly suggesting that NETosis was not induced (Fig. 5B, *enlarged panel*). Of note, endothelial cells were also detected at the site of the injury, confirming that the laser-induced injury model of thrombosis did not result in exposure of the subendothelial matrix or collagen to the bloodstream. Three-dimensional (3D) modeling of the laser-induced thrombus using serial block face (SBF) electron microscopy confirmed our observations: neutrophils observed at the site of injury did not secrete DNA, exhibited intact membranes, and interacted with the injured endothelial cells in one area and platelets contributing to the thrombus in the other area (Fig. 5C). We next used SBF to scan the thrombus core to detect the presence of NETs. To do so, the thrombi obtained following laser injury were analyzed by X-ray microcomputed tomography (micro-CT) with voxel sizes of 5.17 (4 \times) and 0.57 μ m (40 \times) (*SI Appendix, Fig. 1A*) before being examined by SBF. The thrombi were scanned with a step of 100 nm for a length of 40 μ m to reconstruct a 3D image of the core of the thrombus. More than 40,000 images of different fields constituting the thrombus were generated. The results indicated that platelets and red blood cells were present in the core of the thrombus. However, no neutrophils or NETs were detected (*SI Appendix, Fig. 1B and Movie S1*). Taken together, these results indicate that no NETs form *in vivo* following laser-induced injury (*SI Appendix, Fig. 5*).

DNase-I Hydrolyzes ATP and ADP and Generates Adenosine. To determine how DNase-I affects thrombus formation independent of NET formation, we next determined the effect of DNase-I on neutrophil and platelet activation induced by ATP or ADP. We previously demonstrated that ATP and ADP are agonists that play an important role in neutrophil activation and thrombus formation in our model (1). Furthermore, DNase-I is a nuclease that has been shown to preferentially cleave phosphodiester linkages and may thus potentially degrade ATP and ADP (*SI Appendix, Fig. S3*). Compared to that observed after no treatment, the quantity of ATP was decreased by up to 32% following the addition of 25 U of DNase-I (Fig. 6A). Interestingly, neutrophil activation, which was reflected by CD11b expression, was significantly reduced when

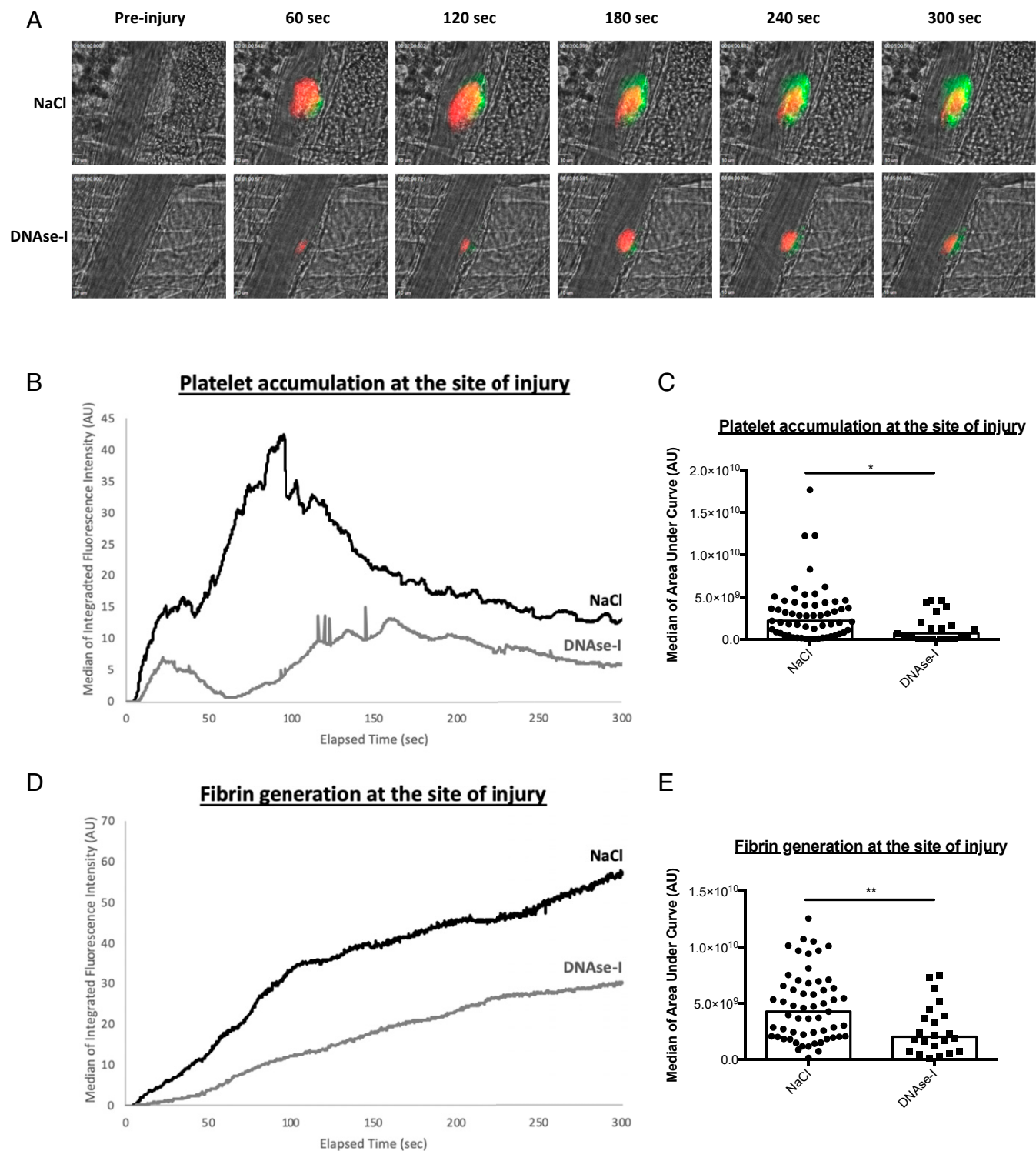


Fig. 1. DNase-I affects thrombus formation and fibrin generation at the site of injury in WT mice. (A) Representative images of thrombus formation and fibrin generation after a laser injury over time in absence (NaCl) or in presence of DNase-I (DNase-I). The thrombus formation was evaluated through platelet accumulation depicted in red (X649, 0.25 μ g/g of mouse). Fibrin generation was detected with Fib-DyLight 488 (0.25 μ g/g of mouse) and represented in green. Blood flow was from the *Top* to the *Bottom*. (B) Graph presents kinetics of platelet accumulation after a laser injury in WT mouse in absence (NaCl, 29 thrombi in three mice) or presence of DNase-I (DNase-I, 22 thrombi in three mice). (C) Graph depicts the medians of area under curve of fluorescent signal corresponding to platelet accumulation in absence (NaCl) or presence of DNase-I (DNase-I) (Mann-Whitney *U* test, * $P < 0.05$). (D) Kinetics of fibrin accumulation after a laser injury in WT mice in absence (NaCl, 29 thrombi in three mice) or in presence of DNase-I (DNase-I, 22 thrombi in three mice). (E) Graph depicts the medians of area under curve of fluorescent signal corresponding to fibrin accumulation after a laser injury in absence (NaCl) or in presence of DNase-I (DNase-I) (Mann-Whitney *U* test, ** $P < 0.01$).

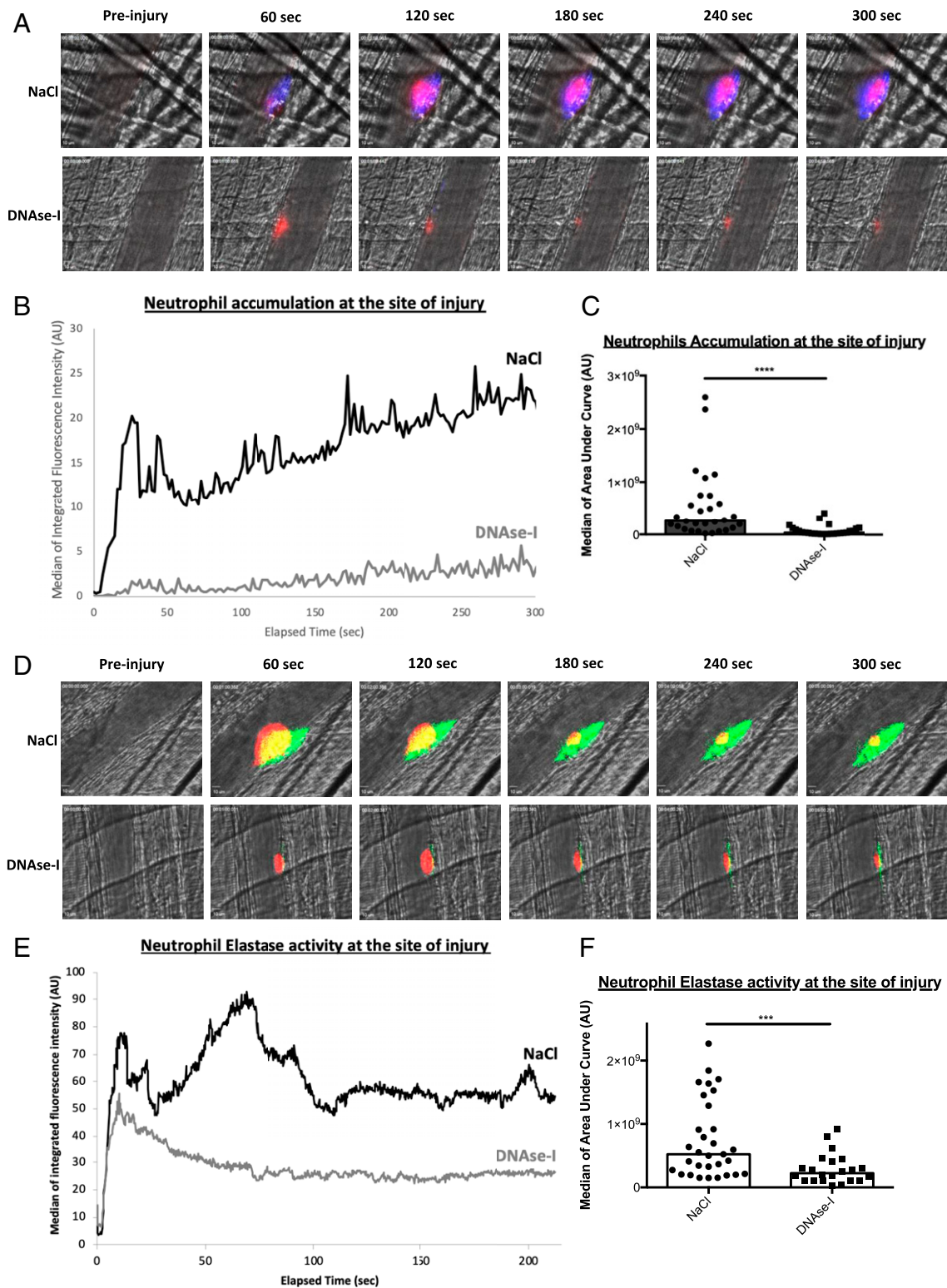


Fig. 2. DNase-I affects neutrophil accumulation and activation at the site of injury in WT mice. (A) Representative images of neutrophil accumulation in arterioles at the site of thrombus formation after a laser injury over time in absence (NaCl, 29 thrombi in three mice) or in presence of DNase-I (DNase-I, 26 thrombi in three mice). Platelets are detected with 0.25 $\mu\text{g/g}$ of mouse of X649 and are depicted in red. Neutrophils are observed with 0.5 $\mu\text{g/g}$ of mouse of Ly6G-PE and are depicted in blue. Blood flow is from the *Top* to the *Bottom*. (B) Graph represents kinetics accumulation of neutrophils in absence (NaCl, black line) or presence of DNase-I (DNase-I, gray line). (C) Graph depicts the medians of area under curve of fluorescent signal corresponding to neutrophil accumulation in absence (NaCl) or presence of DNase-I (DNase-I) (Mann–Whitney *U* test, **** $P < 0.0001$). (D) Representative images of NE activity in arterioles at the site of thrombus formation after a laser injury over time in absence (NaCl, 31 thrombi in three mice) or presence of DNase-I (DNase-I, 22 thrombi in three mice). Platelets are detected with 0.25 $\mu\text{g/g}$ of mouse of X649 and are depicted in red. Neutrophil elastase activity is observed with 0.25 $\mu\text{g/g}$ of mouse of NE activity probe and is depicted in green. Blood flow is from the *Top* to the *Bottom*. (E) Graph represents kinetics of neutrophil elastase activity in absence (NaCl, black line) or presence of DNase-I (DNase-I, gray line). Three mice were performed. (F) Graph depicts the medians of area under curve of fluorescent signal corresponding to neutrophil elastase activity in absence (NaCl) or presence of DNase-I (DNase-I) (Mann–Whitney *U* test, *** $P < 0.001$).

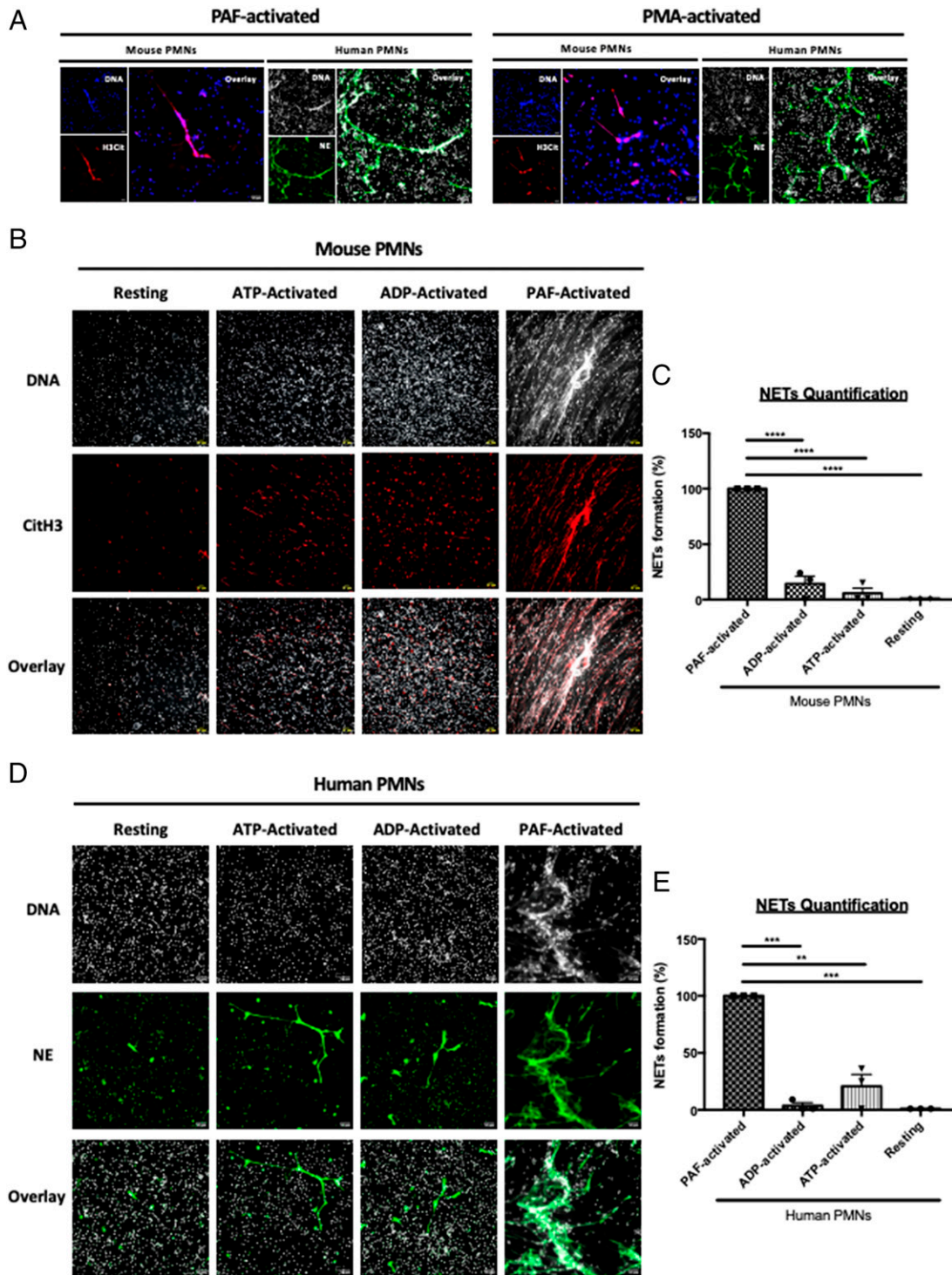


Fig. 3. ATP and ADP participate in neutrophil activation but not in NETs formation. (A) Representative images of PAF-activated (Left Panel) and PMA-activated neutrophils (Right Panel). Purified neutrophils were primed with TNF-alpha and were respectively activated with PAF or PMA for 3 h. After NETosis induction, neutrophils were immunostained with anti-CitH3 antibody (in red) or anti-NE antibody (in green) and Hoechst 33342 for DNA labeling (in gray for human neutrophils or blue for mouse neutrophils). (B) Representative images of CitH3 expression on mouse neutrophils. Purified neutrophils were primed or not with TNF-alpha excepted and activated or not with ATP, ADP, or PAF. Neutrophils were immunostained with anti-CitH3 antibody (in red) and Hoechst 33342 for DNA labeling (in gray). Colocalization of both labeling (DNA/CitH3+) was represented in pink. (C) Graph depicts the percentage of NETs formation from mouse neutrophils in each condition (mean \pm SEM). PAF-activated neutrophils condition was used as positive control corresponding to 100% of NETs formation. (D) Representative images of NE expression on human neutrophils. Human purified neutrophils were primed or not with TNF-alpha and activated or not with ATP, ADP, or PAF. Neutrophils were immunostained with anti-NE antibody (in green) and Hoechst 33342 for DNA labeling (in gray). Colocalization of both labeling (DNA/NE+) was represented in light green. (E) Graph depicts the percentage of NETs formation from human neutrophils in each condition (mean \pm SEM). PAF-activated neutrophils condition was used as positive control corresponding to 100% of NETs formation (ANOVA test, Dunnett multiple comparison, **** $P < 0.0001$). Three independent experiments with a minimum of five fields recorded for each condition.

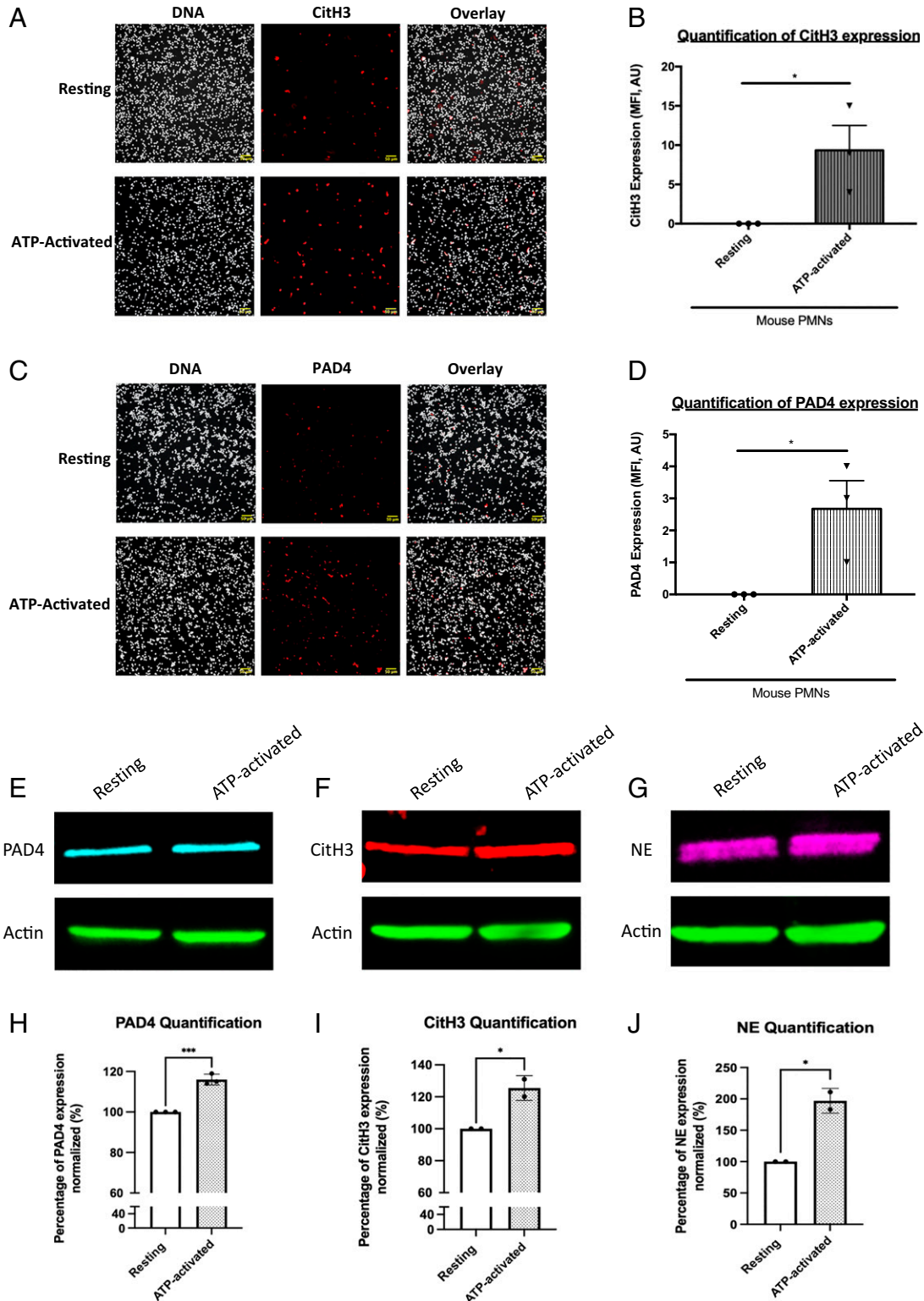


Fig. 4. PAD4, CitH3, and NE are already expressed by resting and ATP-activated neutrophils. (A) Representative images of CitH3 expression on resting and ATP-activated mouse neutrophils. Purified neutrophils were activated with ATP (ATP-activated) or not (resting). Neutrophils were immunostained with anti-CitH3 antibody (in red) and Hoechst 33342 for DNA labeling (in gray). Colocalization of both labeling (DNA/CitH3+) is in pink. (B) Graph depicts the means \pm SEM of neutrophils CitH3+ quantified in each condition (Student's *t* test, $*P < 0.05$). (C) Representative images of PAD4 expression on resting and ATP-activated neutrophils. Neutrophils were immunostained with anti-PAD4 antibody (in red) and Hoechst 33342 for DNA labeling (in gray). Colocalization of both labeling (DNA/PAD4+) is in pink. (D) Graph depicts the means \pm SEM of neutrophils PAD4+ quantified in each condition (Student's *t* test, $***P < 0.01$). Three independent experiments with a minimum of five fields recorded for each condition. (E–G) Western blot analysis of PAD4 (E), CitH3 (F), and NE (G) expression on resting and ATP-activated neutrophils and corresponding statistical analysis. (H–J) Graph depicts the means \pm SEM of PAD4 (H), CitH3 (I), and NE (J) protein quantified in resting and ATP-activated neutrophils (Student's *t* test, $*P < 0.05$, $***P < 0.001$).

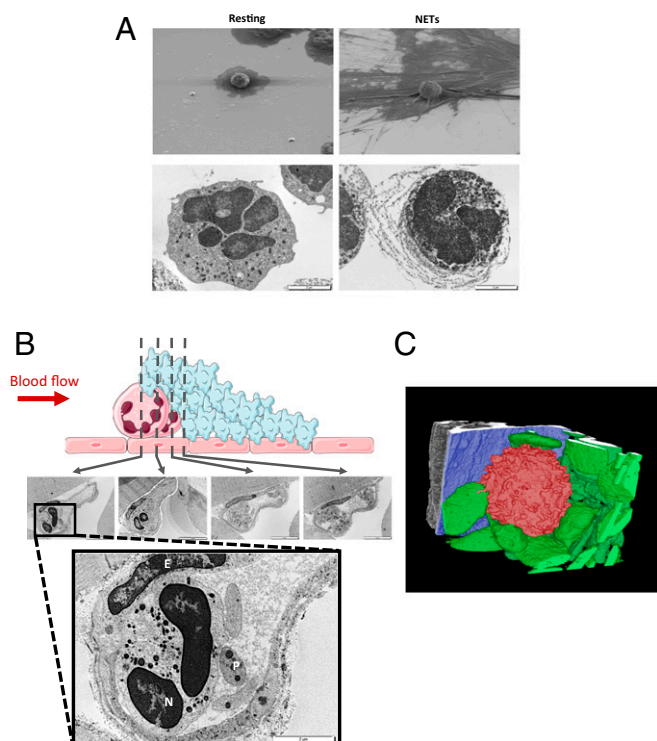


Fig. 5. Neutrophils present at the site of injury do not form NETs. (A) In vitro detection of mice resting neutrophils and NETs induced by PAF (50 μM , 3 h, 37 $^{\circ}\text{C}$) by SEM (Upper Panel) and transmission microscopy (Lower Panel). (B) Representative images of neutrophils present at the site of injury in WT mouse. Neutrophils are upstream to platelet accumulation (Upper Representative Schema). The thrombus was studied by TEM with step of 1 μm . The enlarged picture shows Neutrophil (N), Endothelial Cells (E), and Platelets (P) at the site of injury. (C) 3D modeling representative image of neutrophil (in red) adhering on the activated endothelium (in blue) and interacting with platelets (in green) after a laser injury in a WT mouse.

ATP was incubated with DNase-I compared to when it was left untreated (Fig. 6 G and H).

Similar to the results observed for ATP, DNase-I hydrolyzed ADP, decreasing the quantity of ADP by up to 17% compared to that observed after no treatment (Fig. 6B). The effect of DNase-I on ADP-induced platelet aggregation was even stronger: compared to no treatment, incubation of ADP with DNase-I resulted in a significant reduction in platelet aggregation by up to 49% in the platelet-rich plasma (PRP) of mice (Fig. 6D). These results were confirmed using human PRP (Fig. 6E) and human washed platelets (Fig. 6F), with respectively, 30 and 52% inhibition of platelet aggregation. The inhibition of platelet aggregation by DNase-I was significant when ADP was used between 3 and 10 μM (SI Appendix, Fig. S4). Similarly, compared to no treatment, incubation of ADP with DNase-I resulted in a significant increase in the production of adenosine by up to 28% (Fig. 6C). To confirm the key role played by ATP and ADP on thrombus formation in vivo, we next compared the kinetics of thrombus formation in the Furie model in presence or absence of apyrase. Infusion into a WT mouse of 10 U apyrase (corresponding to a concentration of about 0.005 U/ μL) significantly affects platelet accumulation at the site of injury (Fig. 7 A and B). Altogether, our results indicate that DNase-I inhibits thrombus formation in vivo by hydrolyzing ATP and ADP, two known platelet and neutrophil agonists, leading to the production of adenosine, an inhibitor of neutrophil activation. We previously showed that, following a laser-induced injury, adenosine inhibited neutrophil activation. At the opposite, ATP and ADP are important agonists of neutrophils and platelets (1). To determine the

involvement of ATP in thrombus formation in our model, we next compared the kinetics of platelet accumulation in P2Y12 knock-out (P2Y12 KO) mice treated or not with DNase-I (P2Y12 KO + DNase-I). As expected, platelet accumulation at the site of injury was significantly reduced in P2Y12 KO mice in comparison with WT control mice (Fig. 7 C and D). Interestingly, treatment with 100 U DNase-I in P2Y12 KO mice mostly abolished the thrombus formation (Fig. 7 C and D). We concluded that infusion of DNase-I may also affect in vivo the activation of neutrophils by ATP.

Discussion

Here, we focused our study on the involvement of NETs in arterial thrombosis using the laser-induced model of injury (the “Furie model”). We observed that infusion of DNase-I significantly inhibited thrombus formation in a kinetic incompatible with what was observed in vitro to generate NETs. Indeed, in vitro, to induce NETosis, purified neutrophils are activated using PMA, LPS, and TNF- α for 2 to 6 h. Interestingly, formation of NETs using collagen, vWF, ATP, ADP, and thrombin, all classical agonists of platelets and neutrophils leading to thrombus formation, was never described so far.

Based on our results, we conclude that inhibition of thrombus formation by DNase-I could be independent of NET formation. One of the main difficulties when working with NETs is the lack of a relevant marker for visualizing them. Over the past several years, the presence of CitH3 or PAD4 has been considered a pertinent marker of NETosis. However, more recently, multiple papers have challenged this conclusion. In 2009, Wang et al. showed that citrullination of histones can be detected in activated neutrophils (14). In 2017, Zhou et al. showed that resting viable neutrophils express high levels of PAD enzymes such as PAD2 and PAD4 (15). The authors identified a novel mechanism of extracellular protein citrullination that occurs in the absence of neutrophil apoptosis, necrosis, and NETosis. They demonstrated that enzymatically active PAD4 is expressed on the surface of viable neutrophils and that PAD4 expression on the surface of neutrophils is significantly elevated when neutrophils are stimulated with TNF- α . It was determined that these changes are NETosis independent since the use of diphenylene iodonium (a NETosis inhibitor) has no effect on the up-regulation of PAD4. Following an inflammation, D. Zhang et al., reported the presence of CitH3-positive neutrophil aggregates in mice (16). Here, we confirmed by immunofluorescence and Western blotting that ATP-activated neutrophils express CitH3 and PAD4, confirming that CitH3 and PAD4 are markers of neutrophil activation rather than NET formation. We observed in vitro that neutrophils may express at their surface CitH3, suggesting that activated neutrophils may secrete CitH3 without NET formation. Despite their physiologic nuclear localization, histones have been described to be secreted by dying cells, immune cells (neutrophils, basophils, and mast cells) forming NETs (11, 17) but also LPS- and interferon-activated macrophages (10). It is thus possible that activated neutrophils secrete CitH3, independent of NETosis. The role of CitH3 in thrombosis is, however, to date unknown. We conclude that the role played by NETs and activated neutrophils in different models of thrombosis needs to be reevaluated. The ability to image in vivo NET formation in real-time is necessary to evaluate the presence and role of NETs in thrombus formation.

In the Furie model, neutrophils play a key starter role in the formation of a thrombus. Following the laser-induced injury, the vessel wall gets activated (18), and neutrophils are the first cells to bind to the activated endothelium via LFA-1/ICAM-1 interactions (2). The accumulation of neutrophils at the site of injury is required to induce the formation of a platelet thrombus. Thrombus formation is, in this model, dependent on the TF and independent of the FXII pathway. Neutrophil may represent the main—or the first—source of TF at the site of injury (2). ATP is the main neutrophil activator through P2X1, whereas thrombin, ATP, and ADP constitute the platelet agonists (1, 19–21). We demonstrated

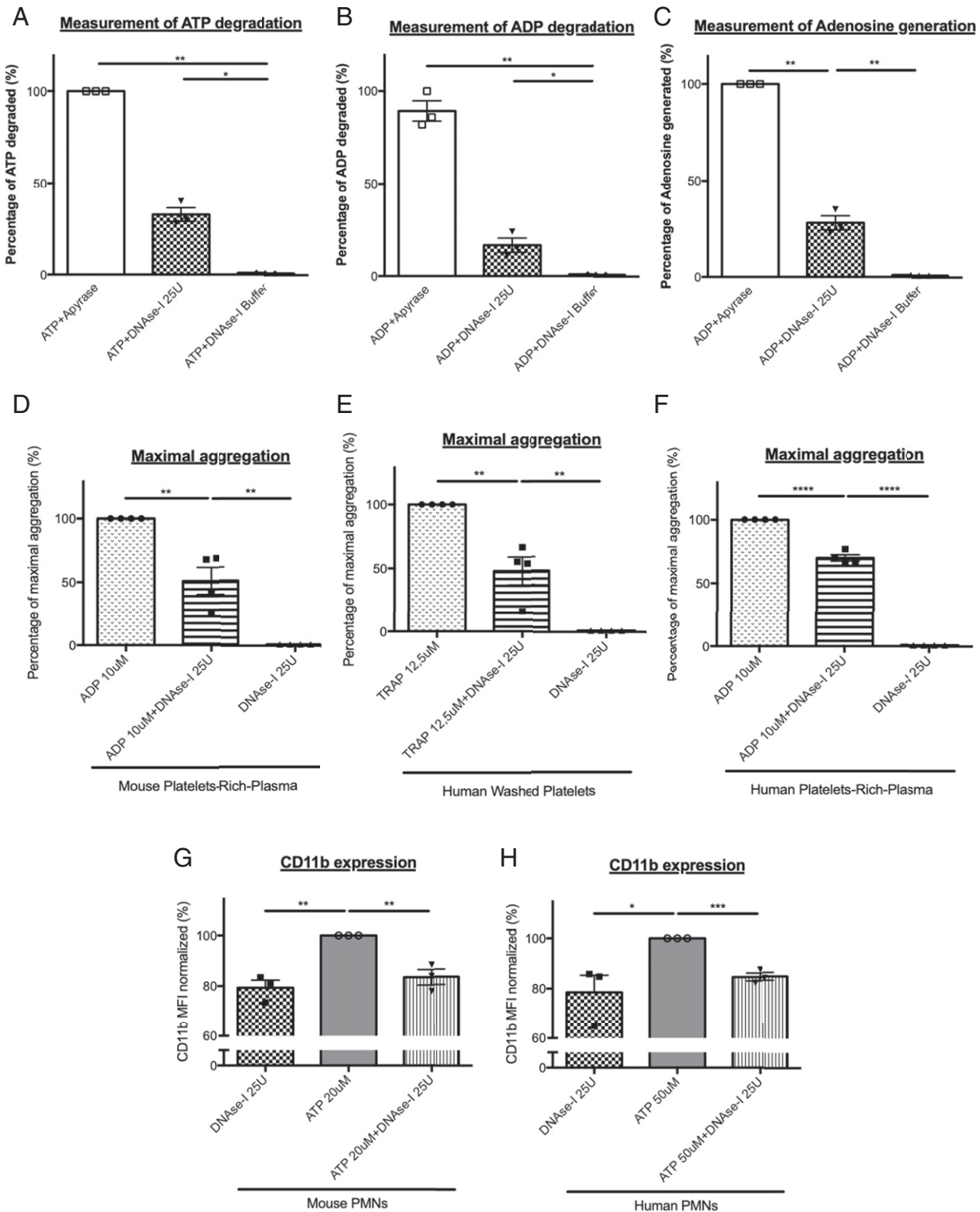


Fig. 6. DNase-I inhibits neutrophil and platelet activation by ATP and ADP degradation. (A and B) ATP or ADP degradation by DNase-I. ATP (A) or ADP (B) was incubated in presence of DNase-I buffer alone (negative control), DNase-I (25 U, 0.25 U/μL), or Apyrase (positive control, 3.5 U, 0.01 U/μL). (C) Production of Adenosine by ADP in presence of DNase-I. ADP was incubated with Apyrase (positive control) or DNase-I. (D and E) Percentage of maximal aggregation after 5 min of mouse (D) or human (E) PRP aggregation. Aggregations were performed in presence of 10 μM ADP or ADP plus DNase-I or in presence of DNase-I alone. (F) Percentage of maximal aggregation after 5 min of human washed platelet aggregation induced by TRAP. Aggregations were performed in presence of 12.5 μM TRAP or TRAP plus DNase-I or in presence of DNase-I alone. (G) Mouse neutrophils CD11b expression after activation with ATP (20 μM) or in presence of ATP plus DNase-I or in presence of DNase-I alone. (H) Human neutrophils CD11b expression after activation with ATP, in presence of ATP plus DNase-I or in presence of DNase-I alone (DNase-I 25 U, negative control) (Student's *t* test, **P* < 0.05, ****P* < 0.001).

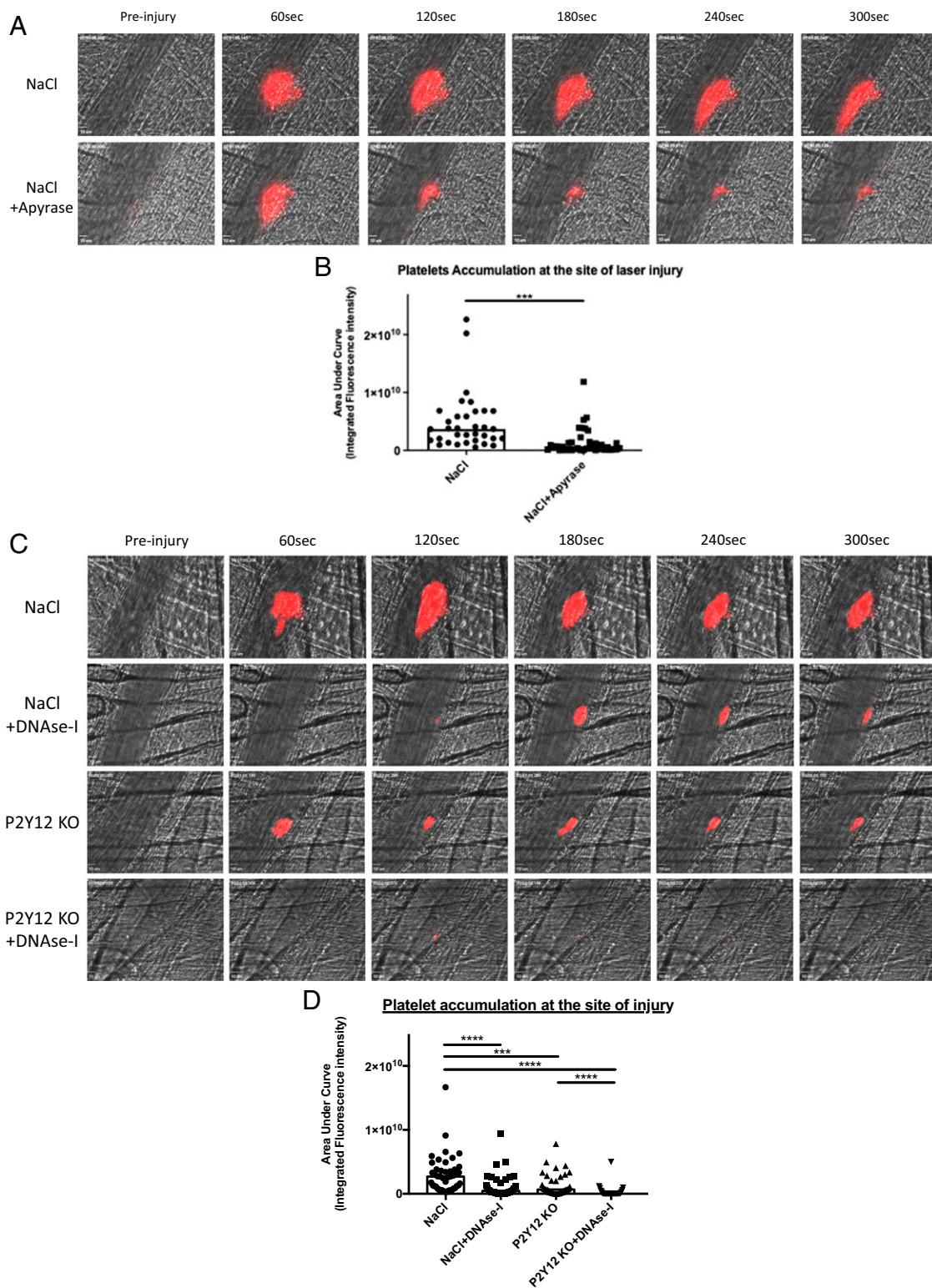


Fig. 7. The model laser of thrombosis is both ATP and ADP dependent. (A) Representative images of thrombus formation after a laser injury overtime in control WT mice (NaCl) and mice injected in Apyrase (NaCl+Apyrase). The thrombus formation was evaluated through platelet accumulation depicted in red. Blood flow was from the *Top* to the *Bottom*. (B) Graph depicts the medians of area under curve of fluorescent signal of platelet accumulation after a laser injury in WT mice (NaCl, 45 thrombi in four mice) and mice injected in Apyrase (NaCl + Apyrase, 32 thrombi in three mice) (Mann-Whitney *U* test, $***P < 0.001$, $****P < 0.0001$). (C) Representative images of thrombus formation after a laser injury overtime in control condition WT mice (NaCl), control mice injected in DNase-I (NaCl + DNase-I), P2Y12 Knockout mice (P2Y12 KO), and P2Y12 Knockout mice injected in DNase-I (P2Y12 KO + DNase-I). The thrombus formation was evaluated through platelet accumulation depicted in red. Blood flow was from the *Top* to the *Bottom*. (D) Graph depicts the medians of area under curve of fluorescent signal of platelet accumulation after a laser injury in WT mice (NaCl, 45 thrombi in four mice), control mice injected in DNase-I (NaCl + DNase-I, 33 thrombi in three mice), P2Y12 KnockOut mice (P2Y12 KO, 38 thrombi in three mice), and P2Y12 Knockout mice injected in DNase-I (P2Y12 KO + DNase-I, 32 thrombi in three mice) (Mann-Whitney *U* test, $***P < 0.001$, $****P < 0.0001$).

that apyrase strongly affects thrombus formation, highlighting the role played by ATP and adenosine on neutrophil accumulation at the site of injury. We propose that DNase-I, by generating adenosine at the site of injury, down-regulates the activation of neutrophils and then their accumulation at the site of injury. Additional studies are required to determine if activation of neutrophil occurs before their binding to the injured endothelium and to identify the signaling pathway explaining how down-regulation by adenosine could prevent the accumulation of neutrophils at the site of injury. Y. Ji et al. have reported that systemic administration of a recombinant apyrase inhibits thrombosis smooth muscle cell migration and intimal hyperplasia in vein grafts without increasing bleeding or compromising re-endothelialization (22). To confirm that point, additional experiments are required to decipher the role played by (ATP-activated) neutrophils in hemostasis. These results suggest, however, that targeting ATP and ADP by using apyrase or DNase-I could represent an original single-drug strategy to prevent thrombosis without affecting hemostasis.

The Furie model is considered as an important model of acute thromboinflammation and could be pertinent to understand the mechanisms leading to thrombosis associated with a polycythemia vera or a solid cancer (23). Here, by electron microscopy, we confirmed our previous observation that collagen is not exposed to the blood circulation since endothelial cells are present at the site of injury. We also observed that neutrophils, interacting with the injured endothelial cells, are present at the site of injury but not in the core of the thrombus. These observations are in perfect adequation with our previous demonstrations that neutrophils are accumulated at the site of injury before platelets and play an important role for thrombin generation. We previously demonstrated that stimulation of the adenosine A_{2A} receptor prevents neutrophil binding, as well as fibrin generation and thrombus formation (2). Similarly, K.E. Barletta et al. have shown that stimulation of the A_{2A} receptor promotes COX-2 and PGE-2 production and inhibits adhesion and infiltration (24). Thus, adenosine mostly prevents platelet activation directly and indirectly through the inhibition of neutrophil activation/accumulation and the production of COX-2 and PGE-2. These results highlight the antithrombotic role of adenosine in thrombosis.

Interestingly, the role of activated endothelium and neutrophils in thrombosis—associated or not with endothelial cell denudation—in the pathogenesis of plaque erosion (25) were also recently point out. NETs are also abundant in coronary thrombi and cerebral occlusions retrieved from patients with acute myocardial infarction (26) and ischemic stroke (27) using histological and immunohistochemical stainings for extracellular DNA, histones, MPO, and NE. However, the role of NETs following a laser-induced injury was so far not studied until now. We observed that DNase-I could synergize with P2Y₁₂ deficiency to more significantly reduce thrombus formation than P2Y₁₂ deficiency alone. We previously observed that neutrophil depletion completely abolished thrombus formation (2), suggesting that neutrophils act as “a starter” to initiate the TF-dependent generation of thrombin required for platelet activation and accumulation at the site of injury. Based on our results, we hypothesized that P2Y₁₂ deficiency will mostly exclusively affect platelet activation to ADP, whereas infusion of DNase-I, by hydrolyzing ATP and ADP, will inhibit both ATP-dependent neutrophil activation and ATP- and ADP-dependent platelet activation. The fact that thrombus formation was significantly reduced in P2Y₁₂ null mice confirms the key role played by ADP on platelets activated by thrombin.

Currently, injecting DNase-I into mice is the main method for demonstrating the role played by NETs in thrombosis. Here, we demonstrated that injection of DNase-I is not sufficient to determine the involvement of NETs in thrombosis, as DNase-I acts on different targets (i.e., ATP and ADP). DNase-I is an endonuclease that has been shown to digest extracellular double-stranded DNA. DNase activity typically requires divalent cations (Ca²⁺ or Mg²⁺)

and leaves 5' phosphates following DNA cleavage. Consistent with this finding, injection of DNase-I has been reported to affect the infarct size in a mouse model of myocardial ischemia/reperfusion injury (28). Furthermore, monotherapy with DNase-I reduces the infiltration and activation of neutrophils, inducing the activation of cardioprotective and anti-inflammatory mechanisms. The effect of DNase-I on inflammation has been confirmed in a mouse model of acute limb ischemia/reperfusion injury (29). Treatment with DNase-I significantly decreases the number of infiltrating inflammatory cells. Altogether, these results indicate that DNase-I may act independently of NET formation and point out the key role played by ATP and ADP in neutrophil activation and thrombus formation following a laser-induced injury.

Methods

Mice. WT CR57Bl/6J mice (5 to 9 wk old) were obtained from Elevage Janvier. All animal care and experimental procedures were performed as recommended by the European Community Guidelines (directive 2010/63/UE) and approved by the Marseille Ethical Committee 14 (protocol: APAFIS#20334-2019041811535225).

Antibodies and Reagents. PE rat anti-mouse Ly6G was obtained from BD Biosciences. Brilliant Violet 421 nm rat anti-mouse CD45 and Alexa Fluor 647 rat-anti-mouse CD11b were obtained from BioLegend. Apyrase from potatoes, ATP, and ADP et ADP Kit were purchased from Sigma-Aldrich. Anti-Ly6G microbeads were obtained from Miltenyi Biotec. RNase-free DNase-I was from Promega. Rabbit anti-mouse CitH3 (clone ab5103), PAD4 (clone ab214810), and Adenosine Kit were obtained from Abcam. ATP Determination Kit was obtained from Life Technologies. The rat anti-mouse GPIb Dylight 649 was obtained from Emfret.

Purification of Mouse Polymorphonuclear Neutrophils. Mouse polymorphonuclear neutrophils (PMNs) were isolated from bone marrow of three mice WT CR57Bl/6J using biotin-coupled magnetic microbeads and biotin anti-Ly6G antibody as described by the manufacturer (Miltenyi Biotec). Briefly, bone marrow was flushed out of femurs using phosphate-buffered calcium-free saline (PBS^{-/-}) supplemented with 0.5% bovine serum albumin (BSA) and ethylenediaminetetraacetic acid, passed through a 30- μ m filter (Miltenyi Biotec) to obtain a single cell solution. After centrifugation, pellet was resuspended, stained with biotin anti-Ly6G antibody for 10 min in the dark at 4 °C and completed with antibiotin microbeads for 15 min. Magnetic immunoseparation of PMNs was performed using LS columns (Miltenyi Biotec). Cells were washed and reloaded in calcium and magnesium with PBS^{+/+}. PMN count was determined using Kova slides, and viability was assessed using the trypan blue coloration. PMN purity was routinely >98% confirmed by flow cytometry using anti-CD45 and -Ly6G antibodies.

Purification of Human PMNs. Blood was obtained from the French Blood institute EFS (“Établissement français du Sang”; agreement Nos. 7829 and 7954). PMNs were isolated with Human StraightFrom Whole Blood CD15 microbeads kits from Miltenyi Biotec. Briefly, after erythrocytes lysis, the blood cells were incubated in the presence of CD15 microbeads. Blood cells were washed with separation buffer and centrifuged at 300 g for 10 min at room temperature. The pellets containing magnetically labeled cells were resuspended in separation buffer and applied to the equilibrated whole blood column placed on the QuadroMACS. After extensive washing, the column was removed from the magnetic separator, and labeled cells were eluted using whole blood elution buffer. Finally, the PMNs were centrifuged at 300 g for 10 min and resuspended in Hank's buffer with calcium and magnesium. The neutrophil purity was verified by flow cytometry based on CD45/CD66b expression and was always higher than 98%.

Flow Cytometry. Analyses of cell surface CD45, Ly6G, and CD11b expression on purified mouse PMNs, and CD45, CD66b, and CD11b expression on purified human PMNs were performed with a flow cytometer (Gallios, Beckman Coulter) using appropriate antibodies. Viability was verified by LiveDead probe use (ThermoFisher). A minimum of 200,000 cells were analyzed for each condition.

In Vitro NET Experiments. After isolation, PMNs were primed with TNF-alpha (2 ng/mL) for 30 min at 37 °C and 5% CO₂. Priming was confirmed by CD11b overexpression determined by flow cytometry. Primed PMNs (1 \times 10⁶ cells) were allowed to adhere to poly-L-lysine-coated slides in a 24-well plate at

37 °C and 5% CO₂ for 1 h. NET formation by adherent PMNs was induced by stimulation with 25 μM PAF (Calbiochem) for 3 h at 37 °C. Then, the cells were fixed with 4% paraformaldehyde for 10 min at room temperature. The PMNs were washed with PBS and blocked with 1% BSA for immunofluorescence staining. The cells were incubated for 1 h 30 min in the dark at 4 °C with an anticitrullinated histone H3 rabbit polyclonal antibody or with an anti-PAD4 rabbit polyclonal antibody. After washing, a secondary rabbit-specific polyclonal antibody conjugated to Alexa Fluor 647 was added to the cells, and the cells were incubated in the dark for 45 min at room temperature.

Intravital Microscopy and Laser-Induced Injury. Intravital video microscopy of the cremaster muscle microcirculation was done as previously described (20). WT mice CR57BL/6J were preanesthetized with intraperitoneal ketamine (100 mg/kg), xylazine (12.5 mg/kg), and atropine (0.25 mg/kg). A tracheal tube was inserted, and the mouse maintained at 37 °C with hot full gloves at proximity. To maintain anesthesia, thiopental (12.5 mg/kg every 30 min) was administered through a cannula placed in the jugular vein. After, the scrotum was incised, and the testicle and cremaster muscle were exteriorized. The cremaster was superfused with thermo-controlled buffer (37 °C).

Vessel wall injury was induced with a nitrogen laser dye (MicroPoint, Photonics Instruments), focused through the microscope's objective and aimed the vessel wall on the cremaster. Typically, one or two pulses were required to induce vessel injury. The first injury was performed 5 to 10 min after the infusion of DNase-I. Multiple thrombi were studied in a single mouse for a period of 2 h with new thrombi formed upstream of earlier thrombi to avoid any contribution from thrombi generated earlier in the animal. Image analysis was performed using SlideBook 6 (Intelligent Imaging Innovations). Fluorescence data were analyzed as previously described to determine the median of fluorescent intensity signal over time.

TEM. Clots induced by laser dye were fixed with paraformaldehyde (PFA) 4%/0.1 M phosphate buffer, pH 7.4, by intracardiac perfusion and cremaster superfusion for 1 h. The cremaster muscle was prepared for TEM by postfixation in OsO₄, dehydration in a graded series of ethanol to absolute ethanol, and embedding in Epon 812 resin. Ultrathin sections (60 nm) were obtained with an ultramicrotome (UltraCut E, Reichert Jung) and stained with 5% uranyl acetate before morphological examination under a transmission electron microscope (JEM 1400 JEOL).

SEM. Primed mouse neutrophils (1 × 10⁶ cells) in 24-well flat-bottom plates were adhered to coverslips treated with poly-L-lysine, and the coverslips were coated with 20 nm gold. The plates were incubated for 3 h in an incubator with 5% CO₂ at 37 °C to induce NETosis. Then, resting neutrophils (not treated with PAF) and NETs (treated with PAF 10 μM) were fixed with 4% PFA/0.1 M phosphate buffer, pH 7.4, for 1 h. After dehydration, the coverslips were coated with 20 nm gold a second time and analyzed under a scanning electron microscope (Quanta 200, FEI).

SBF-SEM. Platelet thrombi induced by laser dye in the mouse arterial microcirculation were fixed using a combination of glutaraldehyde for fixation, ferrocyanide-reduced osmium tetroxide for postfixation, thiocarbonylhydrazide, and osmium tetroxide, followed by uranyl acetate. Then, the samples were dehydrated in a graded series of ethanol to absolute ethanol and acetone and embedded in Durcupan resin. Ultrathin sections (90 nm) were obtained with an ultramicrotome for morphological examination and verification under a transmission electron microscope (Technai G2, Thermo Fisher Scientific). Cremaster muscles with thrombi were mounted on an SBF pin, and acquisition was performed upstream of the blood flow. The samples were visualized with an SEM microscope equipped with a VolumeScope SBF

module (Teneo VS, Thermo Fisher Scientific). Acquisition was carried out at a thickness of 100 nm and a pixel size of 10 nm.

Western Blot Analysis. After collection of mouse or human neutrophils, samples were homogenized in radioimmunoprecipitation assay buffer supplemented with protease and phosphatase inhibitor (Thermo Fisher) on ice. After centrifugation at 10,000 rpm for 30 min at 4 °C, the protein content was determined by protein assay (Thermo Fisher). An equal amount of protein per sample was resolved on gradient gel (4 to 20% Tris-Glycine gels, Thermo Fisher) and then transferred onto nitrocellulose membranes. Each membrane was incubated in blocking buffer for 1 h and incubated with primary antibodies—NE, PAD4, and CitH3—overnight at 4 °C. Reactivity was determined by fluorescence using Alexa Fluor-conjugated secondary antibodies. Images were obtained and quantified using iBright CL1500 and associated software.

Preparation of Mouse PRP and Aggregation Test. Blood was obtained from three WT C57BL/6J mice anesthetized (100 mg/kg ketamine, 25 mg/kg xylazine, and 0.25 mg/kg atropine) and collected on citrated buffer (1 for 9e). Blood was centrifuged and PRP was incubated in the presence of CaCl₂ (2 mM) and MgCl₂ (1 mM) during 30 min at 37 °C. PRP was preincubated at 37 °C in a cuvette on aggregometer. The aggregation assay was started with 0% aggregation baseline. Then, PRP was stimulated by ADP (10 μM) in the presence or absence of DNase-I (25 U). Aggregation test was followed for 5 min.

Preparation of Human Washed Platelets. Blood was obtained from the French Blood institute EFS (agreements 7829 and 7954). Healthy volunteers signed a consent procedure before drawing blood. Blood samples were centrifuged at 200 g for 13 min at 37 °C to obtain PRPs. PRPs were then centrifuged at 900 g for 13 min at 37 °C to obtain platelet pellets. The pellets were carefully resuspended in Tyrode/BSA buffer (138 mM NaCl, 2.9 M KCl, 12 mM NaHCO₃, 0.36 mM NaH₂PO₄, 5.5 mM glucose, 10 mM Hepes, 2% BSA, pH 7.4) supplemented with apyrase (0.02 U/mL) and PGI₂ (0.1 μM) and 1 mM calcium and 1 mM magnesium. Platelets were washed twice in Tyrode/BSA buffer and resuspended in Tyrode/BSA buffer without apyrase nor prostacyclin. Washed platelets were kept at 37 °C for 30 min before used.

Detection of NE Activity In Vivo. NE activity was detected in vivo using BODIPY-FL-labeled DQ-elastin from Life Technologies. Each C57BL/6J WT mouse was infused with 0.25 μg/g BODIPY-FL-labeled DQ-elastin. After laser-induced injury, NE activity was observed by excitation at 488 nm and images were obtained over time points.

Statistical Analysis. Data are representative of at least three independent experiments for all the in vitro experiments. To determine statistical significance, in vitro experiments, significance was determined using the unpaired two-tailed Student's *t* test. For the in vivo experiments, significance was determined using unpaired Mann-Whitney *U* test. Differences were considered significant at *P* < 0.05.

Data Availability. All study data are included in the article and/or supporting information.

ACKNOWLEDGMENTS. We gratefully acknowledge Perrine Chaurand and Daniel Borschneck (Centre Européen de Recherche et d'Enseignement des Géosciences de l'Environnement, Aix-Marseille University) for help localizing thrombi in mouse cremaster by X-ray microcomputed tomography.

1. R. Darbousset et al., P2X1 expressed on polymorphonuclear neutrophils and platelets is required for thrombosis in mice. *Blood* **124**, 2575–2585 (2014).
2. R. Darbousset et al., Tissue factor-positive neutrophils bind to injured endothelial wall and initiate thrombus formation. *Blood* **120**, 2133–2143 (2012).
3. A. Brill et al., Neutrophil extracellular traps promote deep vein thrombosis in mice. *J. Thromb. Haemost.* **10**, 136–144 (2012).
4. T. A. Fuchs, A. Brill, D. D. Wagner, Neutrophil extracellular trap (NET) impact on deep vein thrombosis. *Arterioscler. Thromb. Vasc. Biol.* **32**, 1777–1783 (2012).
5. E. F. Kenny et al., Diverse stimuli engage different neutrophil extracellular trap pathways. *eLife* **6**, e24437 (2017).
6. V. Papayannopoulos, K. D. Metzler, A. Hakkim, A. Zychlinsky, Neutrophil elastase and myeloperoxidase regulate the formation of neutrophil extracellular traps. *J. Cell Biol.* **191**, 677–691 (2010).
7. Y. Zhou et al., Evidence for a direct link between PAD4-mediated citrullination and the oxidative burst in human neutrophils. *Sci. Rep.* **8**, 15228 (2018).
8. T. A. Fuchs et al., Extracellular DNA traps promote thrombosis. *Proc. Natl. Acad. Sci. U.S.A.* **107**, 15880–15885 (2010).
9. T. A. Fuchs, A. A. Bhandari, D. D. Wagner, Histones induce rapid and profound thrombocytopenia in mice. *Blood* **118**, 3708–3714 (2011).
10. J. Xu et al., Extracellular histones are major mediators of death in sepsis. *Nat. Med.* **15**, 1318–1321 (2009).
11. F. Semeraro et al., Extracellular histones promote thrombin generation through platelet-dependent mechanisms: Involvement of platelet TLR2 and TLR4. *Blood* **118**, 1952–1961 (2011).
12. S. Massberg et al., Reciprocal coupling of coagulation and innate immunity via neutrophil serine proteases. *Nat. Med.* **16**, 887–896 (2010).
13. M.-L. von Brühl et al., Monocytes, neutrophils, and platelets cooperate to initiate and propagate venous thrombosis in mice in vivo. *J. Exp. Med.* **209**, 819–835 (2012).
14. Y. Wang et al., Histone hypercitrullination mediates chromatin decondensation and neutrophil extracellular trap formation. *J. Cell Biol.* **184**, 205–213 (2009).

15. Y. Zhou *et al.*, Spontaneous secretion of the citrullination enzyme PAD2 and cell surface exposure of PAD4 by neutrophils. *Front. Immunol.* **8**, 1200 (2017).
16. D. Zhang *et al.*, Neutrophil ageing is regulated by the microbiome. *Nature* **525**, 528–532 (2015).
17. G. Soslau, P. J. Prest, R. Class, M. Jost, L. Mathews, Inhibition of γ -thrombin-induced human platelet aggregation by histone H1subtypes and H1.3 fragments. *Platelets* **20**, 349–356 (2009).
18. B. T. Atkinson *et al.*, Laser-induced endothelial cell activation supports fibrin formation. *Blood* **116**, 4675–4683 (2010).
19. E. R. Vandendries, J. R. Hamilton, S. R. Coughlin, B. Furie, B. C. Furie, Par4 is required for platelet thrombus propagation but not fibrin generation in a mouse model of thrombosis. *Proc. Natl. Acad. Sci. U.S.A.* **104**, 288–292 (2007).
20. C. Dubois, L. Panicot-Dubois, J. F. Gainor, B. C. Furie, B. Furie, Thrombin-initiated platelet activation in vivo is vWF independent during thrombus formation in a laser injury model. *J. Clin. Invest.* **117**, 953–960 (2007).
21. C. Dubois, L. Panicot-Dubois, G. Merrill-Skoloff, B. Furie, B. C. Furie, Glycoprotein VI-dependent and -independent pathways of thrombus formation in vivo. *Blood* **107**, 3902–3906 (2006).
22. Y. Ji *et al.*, Recombinant soluble apyrase APT102 inhibits thrombosis and intimal hyperplasia in vein grafts without adversely affecting hemostasis or re-endothelialization. *J. Thromb. Haemost.* **15**, 814–825 (2017).
23. T. Barbui, G. Finazzi, A. Falanga, Myeloproliferative neoplasms and thrombosis. *Blood* **122**, 2176–2184 (2013).
24. K. E. Barletta, K. Ley, B. Mehrad, Regulation of neutrophil function by adenosine. *Arterioscler. Thromb. Vasc. Biol.* **32**, 856–864 (2012).
25. G. Franck, Role of mechanical stress and neutrophils in the pathogenesis of plaque erosion. *Atherosclerosis* **318**, 60–69 (2021).
26. A. Mangold *et al.*, Coronary neutrophil extracellular trap burden and deoxyribonuclease activity in ST-elevation acute coronary syndrome are predictors of ST-segment resolution and infarct size. *Circ. Res.* **116**, 1182–1192 (2015).
27. E. Laridan *et al.*, Neutrophil extracellular traps in ischemic stroke thrombi. *Ann. Neurol.* **82**, 223–232 (2017).
28. A. S. Savchenko *et al.*, VWF-mediated leukocyte recruitment with chromatin decondensation by PAD4 increases myocardial ischemia/reperfusion injury in mice. *Blood* **123**, 141–148 (2014).
29. H. Albadawi *et al.*, Effect of DNase I treatment and neutrophil depletion on acute limb ischemia-reperfusion injury in mice. *J. Vasc. Surg.* **64**, 484–493 (2016).